Bandwidth study of volume holography in photorefractive InP:Fe for femtosecond pulse readout at 1.5 μm

Y. Ding and D. D. Nolte

Department of Physics, Purdue University, 1396 Physics Building, West Lafayette, Indiana 47907-1396

Z. Zheng, A. Kanan, and A. M. Weiner

School of Electrical and Computer Engineering, Purdue University, West Lafayette, Indiana 47907

G. A. Brost

Air Force Research Lab/SNDR, 25 Electronic Parkway, Rome, New York 13441-4515

Received February 11, 1998; revised manuscript received June 29, 1998

The Bragg selectivity of volume holograms makes them not well suited for many Fourier imaging processing applications in the space domain because they perform the function of a spatial filter and limit the field of view. Similarly, for femtosecond pulse holography they reduce the spectral bandwidth of the diffracted signal. However, we show both theoretically and experimentally that it is much easier in the frequency domain than in the space domain to achieve a large enough diffraction bandwidth of volume holograms for the bandwidth of 100-fs pulses to be used for frequency-domain femtosecond pulse shaping. The experiments were performed by nondegenerate four-wave mixing in photorefractive InP:Fe with femtosecond readout at 1.5 μm. © 1998 Optical Society of America [S0740-3224(98)02010-4]

OCIS codes: 320.5540, 090.7330, 160.5320, 190.5330.

1. INTRODUCTION

The development and the commercial availability of sub-100-fs lasers have extended the bandwidth of optical communications and signal processing into the terahertz range. In these applications, functional waveforms with large bandwidths are often needed and can be achieved by processing the laser output pulses. Fourier filtering in a femtosecond pulse shaper[1] is one technique for processing optical signals in the Fourier domain, for which the optical frequency components of the femtosecond pulse are spatially dispersed by a dispersive element, then modified by a filter, and recombined by an identical dispersive element to form the temporal output with a shaped waveform. Among many filtering masks for femtosecond pulses, such as fixed amplitude and phase masks,[1] liquid-crystal spatial light modulators,[2] and acousto-optical modulators,[3] dynamic holograms are interesting because of their flexibility and the possibility of using them to implement dynamic processing.[4] Photorefractive materials[5] are prominent dynamic holographic media because of their low-intensity requirement for writing holograms and their large refractive-index changes. Among photorefractive materials, ferroelectric crystals such as $BaTiO_3$, $LiNbO_3$, and $KNbO_3$ have large electro-optic coefficients, which lead to strong photorefractivity and high diffraction efficiencies but with slow grating response times of seconds. Because of the strong spatial Bragg selectivity of volume holograms, photorefractive crystals are excellent for high-capacity holographic data storage[6] by use of angular multiplexing and for narrow-band interference filtering,[7] but they are considered as not well suited for implementing Fourier-plane filtering operations in space-domain image processing[8] because the Bragg selectivity performs the function of a spatial filter and limits the field of view.[9,10] Special designs, such as the Galilean telescopic beam compression technique in a joint-transform correlator,[11] had to be used to solve the problem. Even holographic memories experience limitations in storage density owing to the Bragg selectivity when volume holograms are written and read out by lasers with greatly different wavelengths, although this is not a problem for identical write and readout wavelengths.[12]

An application of volume holography of interest to us is to use a volume hologram for spatial patterning of spatially dispersed frequency components within a femtosecond pulse-shaping apparatus. We are particularly interested in the possibility of implementing holographic pulse shaping of 1.5-μm optical pulses in the optical communication band by holograms written at near-infrared wavelengths near 1 μm of cw diode lasers and in the appropriate holographic materials for this application. Reading a hologram at longer wavelengths than the writing wavelength makes holograms less volatile, as was demonstrated in holographic data storage, image processing,[10] real-time holography,[13] and recently spectral holography.[14,15] A key issue for this scheme is whether the volume hologram, written by a cw laser producing a constant hologram period, will have a sufficient Bragg

0740-3224/98/112763-06$15.00

matching bandwidth to diffract the entire spectrum of an incident femtosecond pulse with sufficient diffraction efficiency. Our goal here is to investigate the bandwidth of femtosecond pulses diffracted from volume holograms in photorefractive InP:Fe. Our results elucidate the conditions under which sufficient bandwidth is available to diffract the entire bandwidth of femtosecond pulses and suggest the appropriate candidate materials, the photorefractive semiconductors.

In previous experiments $LiNbO_3$ was used for processing femtosecond pulses in the frequency domain,[16] but because of the concern of Bragg limitation, a short crystal (1 mm) and small incident angles were used, which reduced the diffraction efficiency in this material. The holographic recording time was 1–2 min.[14] Thin holograms such as GaAlAs/GaAs multiple quantum wells, for which the Bragg limitation is eliminated because the diffraction is in the Raman–Nath regime, have been used for femtosecond pulse shaping[17] and time-domain image edge enhancement[18] with a significantly improved response time of several microseconds with input diffraction efficiencies of 10^{-3}, limited by the interaction length.

For volume holograms with large interaction length, the Bragg selection becomes weaker when the incident angle is small or, similarly, if the grating spacing is large. For photorefractive oxides with diffusion as the sole charge transport mechanism, the optimum grating spacing for diffraction is small, typically $\leqslant 1$ μm. For larger grating spacings diffusion results in a decreasing space-charge field as well as a decreasing hologram strength that is inversely proportional to the grating spacing. On the other hand, for photorefractive semiconductors such as GaAs, InP, and CdTe an external electric field is usually applied to enhance the space-charge field as well as the photorefractivity, which is weak without the applied field because of the small electro-optic coefficients. As a result, charge drift becomes the dominant transport mechanism, which moves the optimum grating spacing to a larger value, usually $\geqslant 10$ μm, favoring reduced Bragg-selectivity. In addition, photorefractive semiconductors have much faster response times than ferroelectrics because of their large carrier mobility, and they are sensitive to the wavelengths in the near-infrared that are important for optical communications. These aspects may make the photorefractive semiconductor crystals suitable for femtosecond applications that use Fourier-plane filtering.

In the research described this paper we use photorefractive InP:Fe as the holographic material because it is a prominent photorefractive semiconductor with high two-wave mixing gain.[19,20] Photorefractive phenomena that require high beam-coupling strength, such as self-pumped phase conjugation and double-pumped and double-color-pumped phase-conjugate mirrors,[21] have been observed in InP:Fe at many near-infrared wavelengths including 1.3 μm. However, few studies of photorefractive InP:Fe at 1.5 μm and even fewer with femtosecond pulses have been done. We investigate diffraction of femtosecond pulses at 1.5 μm from volume holograms in InP:Fe both theoretically and experimentally. We demonstrate a diffraction bandwidth of tens of nanometers near 1.5 μm for a 7.8-mm-thick InP:Fe crystal, which is sufficient to accommodate the entire bandwidth of a 100-fs pulse. The result suggests that InP:Fe (and photorefractive semiconductors in general) can be a suitable material for femtosecond pulse processing at 1.5 μm by volume holography within a femtosecond pulse shaper.

2. EXPERIMENTAL SETUP

The experimental setup is shown in Fig. 1, which is a typical transmission hologram write–read geometry. The two hologram writing beams are from a cw diode laser at a wavelength of 980 nm with *s* polarization. The femtosecond probe beam, with a pulse width of 150 fs at 1500 nm, is from an optical parameter oscillator (OPO) pumped by a mode-locked Ti:sapphire laser. The holographic medium is a holographic-cut photorefractive InP:Fe crystal with dimensions of 4.2 mm $\times$ 5.0 mm $\times$ 7.8 mm. The read-out beam is also *s* polarized to yield the maximum diffraction for this crystal orientation.[22] An electric field is applied along the $\langle 001 \rangle$ direction across the 4.2-mm distance. The optical surfaces are the (110) planes with an interaction length $d = 7.8$ mm. The absorption coefficients are 5.2 and 0.08 cm^{-1} at 980 nm and 1.5 μm, respectively, and the corresponding refractive indices are approximately 3.327 and 3.134 at the pump and the reading wavelengths, respectively. The intersection angle $2\theta_p$ of the two writing beams can be changed to yield different grating spacings. To exploit the intensity-temperature resonance in InP:Fe, which leads to a strong refractive-index change,[23] we control the temperature of the crystal with a thermoelectric cooler. The femtosecond probe beam enters the crystal at the Bragg angle for the center wavelength. The diffracted intensity and spectrum are detected by a germanium photodiode (D) and an optical spectrum analyzer.

3. RESULTS AND DISCUSSION

In this section we first give an easy-to-use, analytical expression for diffraction bandwidth for the case of weak diffraction by use of Kogelnik's coupled-wave theory[24] and then discuss the experimental results on diffraction bandwidth of a broadband femtosecond pulse from a volume hologram in a photorefractive crystal.

As is shown in Fig. 1, two copolarized cw write beams at a wavelength of λ_p enter the surface of the photorefractive material at equal angles θ_p (the angles inside the crystal are θ_p'), writing an unslanted photorefractive grating. The grating has the form $\Delta n = \Delta n_0 \cos(Kx)$,

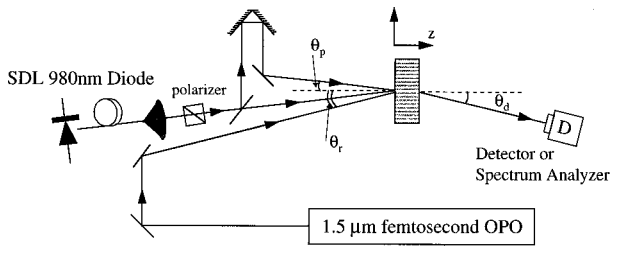

Fig. 1. Experimental setup for diffraction of femtosecond pulses at 1.5 μm from holograms written in photorefractive crystal at 980 nm with a laser diode (SDL) as the hologram writing source and detection of the diffracted signal at the detector (D).

where Δn_0 is the maximum refractive-index change and $K = 2\pi/\Lambda$ is the grating vector length with the grating spacing $\Lambda = \lambda_p/2 \sin \theta_p$. The broadband femtosecond optical reading pulse E_r with a center wavelength of λ_r enters the crystal at an angle of θ_r (the angle inside the crystal is θ_r') and is diffracted by the refractive-index grating. If the absorption is negligible, which is true for an InP crystal at 1.5 μm, and diffraction is weak, the reading beam itself is approximately unaffected. The number of coupled-wave equations in Kogelnik's theory is reduced to one with a constant E_r:

$$\cos\ \theta_r' \frac{dE_d(z)}{dz} - i \frac{K^2\Delta\lambda}{4\pi n_r} E_d(z) = -i\kappa E_r, \qquad (1)$$

where $E_d(z)$ are the electric field of the diffracted beam, $\kappa = \pi\Delta n_r/\lambda_r$ is the coupling coefficient with the amplitude of the refractive-index modulation Δn_r, and $\Delta\lambda = \lambda - \lambda_r$. Here we assume that θ_r' equals the Bragg angle for the center wavelength λ_r. The analytical solution of Eq. (1) for the diffracted field is

$$E_d(z) = -iE_r \frac{8\pi n_r \kappa}{K^2\Delta\lambda} \exp\left(i \frac{K^2\Delta\lambda}{8\pi n_r \cos\ \theta_r'} z\right) \times \sin\left(\frac{K^2\Delta\lambda}{8\pi n_r \cos\ \theta_r'} z\right). \qquad (2)$$

The diffraction efficiency is defined as $\eta = E_d E_d^*/E_r E_r^*$, and the maximum diffraction efficiency η_0 is $(\kappa d/\cos\ \theta_r')^2$ with crystal thickness d. For the broadband read beam incident at an angle θ_r it is impossible for all wavelength components simultaneously to satisfy the Bragg condition. At a wavelength with $\Delta\lambda$ different from λ_r, from Eq. (2), the normalized diffraction efficiency has the form of a squared sinc function:

$$\frac{\eta(\Delta\lambda)}{\eta_0} = \mathrm{sinc}^2\left(\frac{\pi\Delta\lambda d}{2\Lambda^2 n_r \cos\ \theta_r'}\right). \qquad (3)$$

We then get a wavelength range $2\Delta\lambda_{1/2}$, beyond which the diffraction will drop below 50% of its maximum value:

$$\Delta\lambda_{1/2} = 0.886 \frac{\Lambda^2 n_r \cos\ \theta_r'}{d}. \qquad (4)$$

The bandwidth is inversely proportional to grating thickness d, so traditionally it is believed that thick holograms are limited in broadband applications. However, it is also observed that $\Delta\lambda_{1/2}$ depends on the square of the grating period when the changes in the term of $\cos\ \theta_r'$ can be overlooked (which can be done at small incident angles). With increasing grating period, the spectral bandwidth increases rapidly, as our results verify experimentally. In addition, the maximum diffraction efficiency η_0 is independent of grating period, again assuming small angles where $\cos\ \theta_r'$ remains near unity. Therefore one expects to be able to achieve large diffraction bandwidth without sacrificing diffraction efficiency.

With Eq. (3) for the case with a finite incident spectrum $|E_{IN}(\lambda)|^2$, which matches the results given in Ref. 24 under the condition of low conversion efficiency, the output power spectrum is given by $|E_{out}(\lambda)|^2 = \eta_0 \eta(\Delta\lambda) \times |E_{IN}(\lambda)|^2$, which we use to calculate the diffraction output bandwidth and spectrum under our experimental conditions.

Before the femtosecond probe beam is sent to the crystal for the diffraction experiment, the hologram written in the InP:Fe crystal at 980 nm is characterized and optimized by a two-beam coupling experiment in which the energy exchange between the two writing beams is measured. The two-beam coupling gain coefficient is defined as $\Gamma = \ln[\beta r/(1 + \beta - r)]/d$, with beam ratio β and two-beam coupling gain $r = (I_1 \text{ with } I_2)/(I_1 \text{ without } I_2)$ with the beam intensities $I_{1,2}$ measured after the crystal. To achieve an optimum gain, we align the beam path of the two beams to be equal. The FWHM of the peak in the two-beam coupling gain as a function of the delay of one beam is 1.3 mm. Therefore the delay between the two writing beams is set to a precision of a few hundred micrometers for our diffraction experiments.

At excitation wavelengths near 1 μm in InP:Fe the dominant optically excited charges are holes, whereas the thermally excited charges are predominantly electrons. The maximum modulation of the space-charge field as well as of the refractive index is obtained when the dc part in the spatially modulated photocarriers is balanced by the thermally excited charges (electrons). This is called intensity-temperature resonance.[23] For our experiment at an applied field of 6 kV/cm the optimum two-beam coupling gain at an intensity of 60 mW/cm^2 is obtained at a sample temperature of 10 °C with a value of 0.48 cm^{-1} for equal incident intensities of the two beams. The grating spacing is 7.3 μm. Using the relation between the two-beam coupling coefficient and the refractive index change in the crystal $\Gamma = 4\pi\Delta n/\lambda_p$, we can estimate the refractive-index change to be $\Delta n \sim 4 \times 10^{-6}$, assuming a $\pi/2$ phase shift between the refractive-index grating and the intensity grating, which is true under conditions of intensity-temperature resonance.[23] It is not our intention here to achieve high two-beam coupling gain. The small gain value here is caused by the large absorption at the 980-nm pump wavelength, which leads to a strong decrease of intensity in the crystal. As a result, the intensity-temperature resonance cannot be maintained along the crystal for a uniform sample temperature. At longer wavelengths relative to 980 nm, for example at 1.064 or 1.3 μm, the gain coefficient can be increased by at least an order of magnitude.[20,25]

For the diffraction experiment the femtosecond probe beam is incident upon the hologram at the Bragg angle. The measured diffraction efficiency is approximately 10^{-3}, which agrees with the value estimated from Δn in the two-beam coupling experiment. As a femtosecond pulse with a bandwidth of 16 nm enters the crystal, the diffracted spectrum is narrowed by the Bragg selectivity at a small grating spacing. Figure 2 shows the diffraction spectra from holograms with grating spacings of 4.1 and 13.9 μm, corresponding to grating writing angles of 6.9 and 2.0 deg, respectively. The FWHM of the diffraction spectrum at the grating spacing of 4.1 μm has a value of 8 nm, which is half of the incident spectrum width, whereas the value at 13.9 μm is 16 nm, which is equal to the input bandwidth. An experiment was also performed with a 7.3-μm grating period, and an output

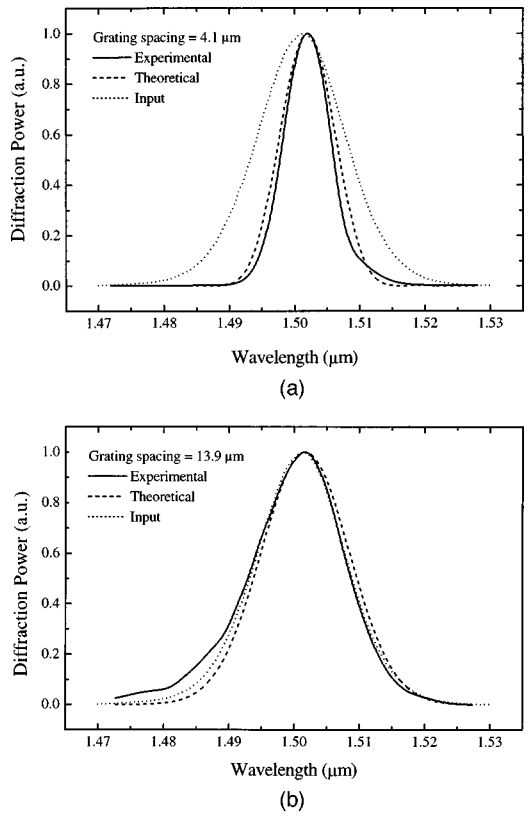

Fig. 2. Experimental diffraction spectra from holograms with grating spacings of 4.1 μm and 13.9 μm (solid curves). The theoretical calculations at these grating spacings and the spectra of the incident pulses are shown for comparison.

bandwidth of 11 nm was observed. Numerical calculations using the Kogelnik theory for these grating spacings are also given in Fig. 2, and they agree well with the experimental data. The spectrum of the input pulse is also plotted in the figure for comparison. Figure 3 shows the theoretical calculation of the bandwidth of the diffracted pulse as a function of the grating spacing with a crystal length ranging from 4 to 11 mm, assuming as before an input pulse with 16-nm bandwidth. At grating spacings larger than 10 μm the entire bandwidth of 16 nm can be reconstructed, even for the 11-mm-thick crystal. Therefore large bandwidth can be obtained at large grating spacings. Although this argument can also be made for the trend in spatial bandwidth, the increase of spectral bandwidth with increasing grating spacing or decreasing incident angle is more rapid. This phenomenon can be seen qualitatively from the rules of thumb for the angular and spectral half-power bandwidth given by Kogelnik, $2\Delta\theta_{1/2} \sim \Lambda/d$ and $2\Delta\lambda/\lambda_{1/2} \sim \cot\theta_r\Lambda/d$, which increases more rapidly than $2\Delta\theta_{1/2}$ with decreasing θ_r.

The crystal thickness is an important parameter in addition to the grating spacing for determining whether a hologram is in the thick or the thin grating regime by use of the Q factor,[26] $Q = 2\pi d\lambda_r/\Lambda^2 n_r$. When $\Lambda = 4.1$ μm, we have $Q \approx 1400$ for a 7.8-mm-thick crystal. This Q value is much larger than 1, indicating that the grating is a thick grating, and the angular selectivity is $2\Delta\theta_r \approx \Lambda/d = 0.03$ deg.[14] At $\Lambda = 14$ μm these values become $Q \approx 117$ and $2\Delta\theta_r \approx 0.1$ deg. Although the grating is still in the thick grating regime under the definition of Q, the bandwidth of the grating diffraction is already large enough for the full spectrum of a 100-fs pulse to be reconstructed in the hologram readout. Figure 4 shows the output bandwidth as a function of the grating spacing with an infinite input bandwidth for a crystal length of 7.8 mm. A pulse with a bandwidth as large as 140 nm was obtained from the diffraction at a grating spacing of 14 μm, which is an appropriate grating spacing for a strong hologram in a photorefractive semiconductor with an applied electric field. Such a bandwidth corresponds to an ultrashort pulse with a pulse width of only 24 fs, assuming a transform-limited Gaussian pulse shape. For those pulses, however, the dispersion of the bulk materials will become much greater. The limit in the hologram thickness is the group-velocity dispersion, which broadens the femtosecond pulse. For InP, the wavelength dependence of the refractive index at room temperature is given by[27]

$$n^2(\lambda) = A + \frac{B\lambda^2}{\lambda^2 - C^2}, \tag{5}$$

where $A = 7.225$, $B = 2.316$, $C^2 = 0.3922 \times 10^8$, and λ is in angstroms (1 Å = 0.1 nm). At 1.5 μm the group-velocity dispersion parameter is $\beta_2 = \lambda^3/2\pi c^2(d^2n/d\lambda^2) = 1880$ ps^2/km. When a Gaussian pulse with an intensity FWHM of t_0 propagates through an InP crystal with a thickness of d, its pulse width is broadened to[28]

$$t_1 = t_0\left[1 + \left(\frac{d}{L_D}\right)^2\right]^{1/2}, \tag{6}$$

with the dispersion length $L_D = 0.36t_0^2/|\beta_2|$. Figure 5 shows the pulse width and the diffraction efficiency as a function of the crystal length for three incident pulse widths. The diffraction efficiency is calculated from the two-wave mixing gain coefficient[25] of 5 cm^{-1} at 1.3 μm. From Eq. (6) and Fig. 5, the crystal length for keeping the broadening less than 20% is 2 cm for a typical 400-fs fiber laser pulse, 3 mm for a typical 150-fs pulse from an optical parametric oscillator, and only 50 μm for a 20-fs pulse. The diffraction efficiency at a crystal thickness of 3 mm would be 14% for the 150-fs pulses. Because of their potential for large bandwidth and their large diffraction efficiency, photorefractive volume holograms in semiconductors are appropriate for applications of Fourier

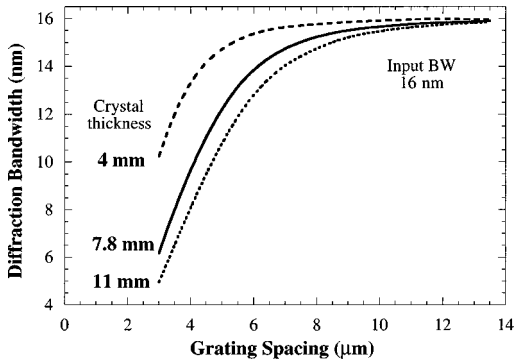

Fig. 3. Bandwidth of the diffracted pulse as a function of the grating spacing with crystal lengths of 4, 7.8, and 11 mm. BW, input bandwidth.

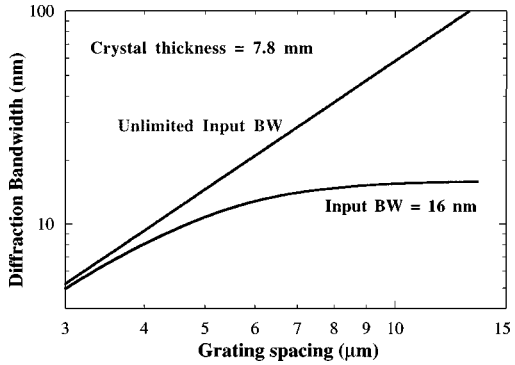

Fig. 4. Output bandwidth as a function of the grating spacing with an infinite input bandwidth (Unlimited Input BW) compared with a 16-nm input bandwidth for a 7.8-mm long crystal, showing large potential bandwidths at large grating spacings for frequency filtering applications.

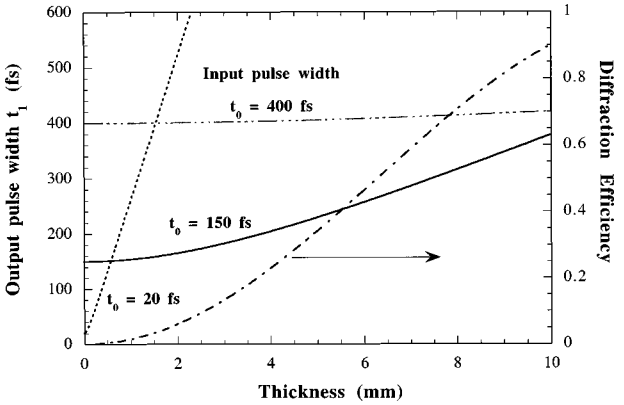

Fig. 5. Calculated pulse width (FWHM) and diffraction efficiency as a function of InP crystal thickness for input pulse widths of 400, 150, and 20 fs at 1.5 μm.

manipulation in the frequency domain, such as pulse shaping, processing, and spectral holography.

4. CONCLUSIONS

In conclusion, we have performed diffraction measurements by using femtosecond 1.5-μm pulses from holograms written by 980-nm cw light in a bulk photorefractive InP:Fe crystal. We have shown that increasing the grating spacing can easily increase the diffraction bandwidth of the hologram in the frequency domain such that it accommodates the entire bandwidth of tens of nanometers of 100-fs laser pulses at 1.5 μm. Our experiments support the practicality of using bulk photorefractive semiconductor crystals such as InP:Fe for dynamic Fourier filtering in the frequency domain for pulses as short as 100 fs. Together with spectral holography, use of these crystals permits dynamic femtosecond waveform processing for ultrafast optic communications applications such as time-reversal, correlation, edge enhancement, and dispersion compensation, with a potentially higher efficiency than by use of holographic thin films.[17,18]

ACKNOWLEDGMENTS

The authors gratefully acknowledge support from the U.S. Department of Defense Focused Research Initiative through U.S. Air Force Office of Scientific Research grant F49620-95-1-0533, National Science Foundation grant 9708230-ECS, and Rome Laboratory award F30602-96-2-0114.

REFERENCES

1. A. M. Weiner, J. P. Heritage, and E. M. Kirschner, "High resolution femtosecond pulse shaping," J. Opt. Soc. Am. B **5**, 1563 (1988).
2. A. M. Weiner, D. E. Leaird, J. S. Patel, and J. R. Wullert II, "Programmable shaping of femtosecond optical pulses by use of a 128-element liquid crystal phase modulator," IEEE J. Quantum Electron. **28**, 908 (1992).
3. C. Hillegas, J. X. Tull, D. Goswami, D. Strickland, and W. S. Warren, "Femtosecond laser pulse shaping by use of microsecond radio-frequency pulses," Opt. Lett. **19**, 737 (1994).
4. K. Ema, "Real-time ultrashort pulse shaping and pulse shape measurement using a dynamic grating," Jpn. J. Appl. Phys., Part 2 **30**, L2046 (1991).
5. P. Günter and J. P. Huignard, *Photorefractive Materials and Their Applications* (Springer-Verlag, Berlin, 1988, 1989), Vols. 1 and 2.
6. J. Heanue, M. Bashaw, and L. Hesselink, "Optical memories implemented with photorefractive media," Opt. Quantum Electron. **25**, S611 (1993).
7. R. Muller, M. T. Santos, L. Arizmendi, and J. M. Cabrera, "A narrow-band interference filter with photorefractive $LiNbO_3$," J. Phys. D **27**, 241 (1994).
8. R. A. Athale and K. Raj, "Fourier-plane filtering by a thick grating: a space–bandwidth analysis," Opt. Lett. **17**, 880 (1992).
9. M. G. Nicholson, I. R. Cooper, M. W. McCall, and C. R. Petts, "Simple computational model of image correlation by four-wave mixing in photorefractive media," Appl. Opt. **26**, 278 (1987).
10. L. Pichon and J. P. Huignard, "Dynamic joint-Fourier-transform correlator by Bragg diffraction in photorefractive $Bi_{12}SiO_{20}$ crystals," Opt. Commun. **36**, 277 (1981).
11. F. T. S. Yu, S. Wu, S. Rajan, and D. A. Gregory, "Compact joint transform correlator with a thick photorefractive crystal," Appl. Opt. **31**, 2416 (1992).
12. J. F. Heanue, M. C. Bashaw, and L. Hesselink, "Volume holographic storage and retrieval of digital data," Science **265**, 749 (1994).
13. D. D. Nolte, Q. N. Wang, and M. R. Melloch, "Robust infrared gratings in photorefractive quantum wells generated by an above-band-gap laser," Appl. Phys. Lett. **58**, 2067 (1991).
14. K. Oba, P. C. Sun, and Y. Fainman, "Nonvolatile photorefractive spectral holography for time domain storage of femtosecond pulses," in *Conference on Lasers and Electro-Optics*, Vol. 11 of 1997 OSA Technical Digest Series (Optical Society of America, Washington, D.C., 1997), pp. 213–214.
15. K. Oba, P. C. Sun, and Y. Fainman, "Nonvolatile photorefractive spectral holography," Opt. Lett. **23**, 915 (1998).
16. P. C. Sun, Y. T. Mazurenko, W. S. C. Chang, P. K. L. Yu, and Y. Fainman, "All-optical parallel-to-serial conversion by holographic spatial-to-temporal frequency encoding," Opt. Lett. **20**, 1728 (1995).
17. Y. Ding, R. M. Brubaker, D. D. Nolte, M. R. Melloch, and A. M. Weiner, "Femtosecond pulse shaping by dynamic holograms in photorefractive multiple quantum wells," Opt. Lett. **22**, 718 (1997).
18. Y. Ding, D. D. Nolte, M. R. Melloch, and A. M. Weiner, "Real-time edge-enhancement of time-domain images," Opt. Lett. **22**, 1101 (1997).
19. J. E. Millerd, S. D. Koehler, E. M. Garmire, A. Partovi, and A. M. Glass, "Photorefractive gain enhancement using band-edge resonance and temperature stabilization," Appl. Phys. Lett. **57**, 2776 (1990).
20. H. J. Eichler, Y. Ding, and B. Smandek, "Two-wave mixing

in InP:Fe at 1064 nm by linear and quadratic photorefractive effect," Opt. Commun. **94**, 127 (1992).
21. N. Wolffer, P. Gravey, G. Picoli, and V. Vieux, "Double phase conjugated mirror and double color pumped oscillator using band-edge photorefractivity in InP:Fe," Opt. Commun. **89**, 17 (1992).
22. Y. Ding and H. J. Eichler, "Crystal orientation dependence of the photorefractive four-wave mixing in compound semiconductors of symmetry group $\bar{4}3m$," Opt. Commun. **110**, 456 (1994).
23. G. Picoli, P. Gravey, C. Ozkul, and V. Vieux, "Theory of two-wave mixing gain enhancement in photorefractive InP:Fe: a new mechanism of resonance," J. Appl. Phys. **66**, 3798 (1989).
24. H. Kogelnik, "Coupled wave theory for thick hologram gratings," Bell Syst. Tech. J. **48**, 2909 (1969).
25. C. Ozkul, G. Picoli, P. Gravey, and N. Wolffer, "High gain coherent amplification in thermally stabilized InP:Fe crystals under dc fields," Appl. Opt. **29**, 2711 (1990).
26. H. J. Eichler, P. Günter, and D. W. Wohl, *Laser-Induced Dynamic Gratings* (Springer-Verlag, Berlin, 1986).
27. O. J. Glembocki and H. Piller, in *Handbook of Optical Constants of Solids*, E. D. Palik, ed. (Academic, Orlando, Fla., 1985), p. 503.
28. G. P. Agrawal, *Nonlinear Fiber Optics*, 2nd ed. (Academic, New York, 1995), p. 65.